Factors Predicting Tracer Uptake in Somatostatin Receptor and MIBG Scintigraphy of Metastatic Gastroenteropancreatic Neuroendocrine Tumors

Samer Ezziddin, MD[1]; Timur Logvinski, MD[1]; Charlotte Yong-Hing, MD[2]; Hojjat Ahmadzadehfar, MD[1]; Hans-Peter Fischer, MD[3]; Holger Palmedo, MD[1]; Jan Bucerius, MD[1]; Michael J. Reinhardt, MD[1]; and Hans-Jürgen Biersack, MD[1]

[1]*Department of Nuclear Medicine, University of Bonn, Bonn, Germany;* [2]*Department of Diagnostic Imaging, University of Alberta, Edmonton, Alberta, Canada; and* [3]*Department of Pathology, University of Bonn, Bonn, Germany*

Radiolabeled octreotide analogs (Oct) and metaiodobenzylguanidine (MIBG) offer 2 different approaches for imaging and targeting metastatic gastroenteropancreatic neuroendocrine tumors (GEP-NET). Despite successful establishment of the revised World Health Organization (WHO) classification, which distinguishes between low- and high-grade malignant GEP-NET, there is a lack of scintigraphic studies comparing uptake behavior on the basis of this categorization. This study aims to define predisposing factors of tracer uptake for both imaging principles implementing the updated tumor criteria of the current WHO classification. **Methods:** Fifty-seven consecutive patients with histologically confirmed metastatic GEP-NET evaluated with both ^{111}In-pentetreotide and ^{123}I/^{131}I-MIBG scintigraphy were included in this study. Intensity of tracer uptake was graded according to the different metastatic regions. Patients were classified as overall positive when avid uptake in the clinically relevant tumor lesions was present. Correlation was tested between the proportion of positive patients and tumor origin, function, and malignancy. **Results:** Overall, 52 patients (91.2%) were Oct positive and 28 patients (49.1%) were MIBG positive. The proportion of tracer-positive patients was significantly higher ($P < 0.05$) in low-grade malignant tumors for both tracers and in functioning as well as in gastroenteral NET for MIBG. Five patients were negative for both tracers. None of the Oct-negative patients proved to be MIBG positive. **Conclusion:** Oct affinity is observed with high frequency throughout the subgroups of metastatic GEP-NET, whereas corresponding MIBG uptake is overall less prevalent and more group dependent. Tumor differentiation significantly impacts both Oct and MIBG uptake, whereas functionality predisposes only for MIBG accumulation. Though clearly inferior to Oct-based radioimaging in most GEP-NET, MIBG achieves a remarkable rate of radioligand accumulation in functioning midgut enterochromaffin cell metastases (>80% of patients positive). These results may have implications for patient management and potentially for selection and performance of targeted therapy.

Key Words: somatostatin receptor scintigraphy; ^{123}I-MIBG; ^{131}I-MIBG; ^{111}In-pentetreotide; gastroenteropancreatic neuroendocrine tumors

J Nucl Med 2006; 47:223–233

Neuroendocrine tumors (NET) present a dedicated field for molecular imaging and nuclear medicine therapy (*1*). Common features, including overexpression of receptors for regulatory peptides such as somatostatin and the presence of cellular structures for amine uptake and storage, allow targeted NET imaging and therapy (*1,2*). The gastroenteropancreatic (GEP) endocrine system represents a large diverse endocrine organ with at least 15 different cell types (*3*). Tumors originating from these cells constitute the heterogeneous entity of GEP-NET, which has a variety of clinicopathologic aspects and an overall incidence of 3–4.5 per 100,000 (*4*). Tumor characterization of the revised World Health Organization (WHO) classification reflects the growing insight into endocrine cell biology and pathology (*5,6*) and has successfully been implemented in the clinical work-up and patient management of GEP-NET. Although the individual clinicopathologic profile based on this WHO classification provides therapeutic and prognostic implications (*7–9*), there is a lack of scintigraphic studies comparing tracer uptake behavior in light of this categorization, which distinguishes between low- and high-grade malignant GEP-NET.

Radiolabeled metaiodobenzylguanidine (MIBG) and octreotide analogs (Oct) provide 2 different approaches to imaging and treating neuroendocrine tumors, using a metabolic versus a receptor-targeted route (*10*). Whereas MIBG uses active transport and concentration mechanisms to accumulate within the tumor cells, the octreotide analog chelator radionuclide complex traps within the tumor cell lysosome after somatostatin receptor–induced internalization (*10,11*). The differing mechanisms of radioligand accumulation may imply differing impacts of tumor cell characteristics on the

Received Jul. 8, 2005; revision accepted Nov. 10, 2005.

For correspondence or reprints contact: Samer Ezziddin, MD, Department of Nuclear Medicine, University Hospital Bonn, Sigmund-Freud-Strasse 25, 53115 Bonn, Germany

E-mail: samer.ezziddin@ukb.uni-bonn.de

TABLE 1
Patient Characteristics, Tumor Localizations, and Tracer Uptake

Patient no.	Age (y)	Sex	Tumor features	Primary site	Location of tumor lesions	Oct uptake	MIBG uptake
1	72	F	LGM, EC-type, F	Ileum	Liver (m), mesent LN (m), pulm (m), bone (m)	+++ (all; except bone ++/+++)	+++ (all; except bone ++/+++)
2	73	M	LGM, EC-type, F	Small bowel	Liver (m), primary (s)	+++	+++
3	66	F	LGM, EC-type, F	Ileum	Liver (m), mesent (s)	+++	+++
4	55	M	LGM, EC-type, F	Small bowel	Liver (m), mesent (s)	+++	+++ (liver), + (mesent)
5	67	F	LGM, EC-type, F	Ileum	Liver (m)	+++	+++
6	47	F	LGM, EC-type, F	NK	Liver (3)	+++	+++
7	53	M	LGM, EC-type, F	Rectum	Liver (m)	+++	+++
8	57	M	LGM, EC-type, F	Ileum	Liver (m), mesent (m)	+++ (liver), ++/− (mesent)	+++ (liver), − (mesent)
9	21	M	LGM, EC-type, F	Ileum	Liver (m), inguinal LN (s)	+++	—
10	62	M	LGM, NF	NK	Liver (m), bone (m)	+++	+++
11	57	F	LGM, EC-type, F	Ileum	Liver (2)	+++	+++
12	34	F	LGM, NF	NK	Liver (m), mesent (m), pancr (s)	+++	+++
13	56	F	LGM, NF	Ileum	Liver (m)	+++	—
14	43	M	LGM, EC-type, F	Ileum	Liver (m)	+++	+++
15	78	F	LGM, EC-type, F	Ileum	Liver (m), bone (m)	+++ (liver), ++ (bone)	++ (liver), +++ (bone)
16	62	M	LGM, EC-type, F	Small bowel	Liver (m), mesent (s)	+++	+++ (liver), ++ (mesent)
17	59	M	LGM, EC-type, F	Colon	Liver (m), colon (s)	+++	++ (colon), − (liver)
18	70	M	LGM, NF	NK	Liver (m), bone (4)	+++ (liver), ++ (bone)	+++ (liver), ++ (bone)
19	77	M	LGM, EC-type, F	NK	Mesent (2)	+++	+++
20	54	F	LGM, NF	Jejunum	Mesent (2)	+++	+++
21	65	F	LGM, EC-type, F	Jejunum	Mesent (s)	++	—
22	71	M	LGM, NF	Ileum	Mesent (s)	+++	+++
23	63	M	LGM, NF	Small bowel	Abdom LN (2), large mesenteric mass (s)	+++	+++ (mesent), ++ (abdom LN)
24	75	M	LGM, NF	Small bowel	Mesent (s)	++	+
25	64	M	LGM, NF	Jejunum	Mesent LN (2)	++	++
26	60	M	LGM, EC-type, F	Ileum	Bone (m)	+++/++	—
27	40	F	LGM, EC-type, F	Bronchus	Mediast LN (s)	+++	+++
28	52	M	LGM, NF	Duodenum	Liver (m), mesent LN (s), primary tumor (s)	− (liver), ++ (LN), +++ (primary)	—
29	62	F	LGM, EC-type, F	Cecum	Liver (m)	+++	+++
30	63	M	LGM, EC-type, F	NK	Liver (2), mesent LN (s)	+++ (liver), ++ (LN)	+++ (liver), ++ (LN)
31	61	M	LGM, NF	Cecum	Liver (m)	+++	+
32	59	F	HGM, NF	Rectum	Liver (m), mediast LN (m)	+++ (LN), − (liver)	—
33	56	M	LGM, NF	Rectum	Liver (m), pulm (s)	+++	—
34	79	F	HGM, NF	Rectum	Liver (m)	++/+++	+/++
35	49	M	LGM, NF	Rectum	Local recurrence (s), pelvic LN (m)	+ (local retrop), − (LN)	+ (local retrop), − (LN)
36	60	M	LGM, NF	Rectum	Liver (m), local (rectum)	+++	—
37	39	F	HGM, NF	NK	Liver (m), bone (4)	+++	—
38	69	M	HGM, NF	NK	Retrop pelvic and inguinal LN (m)	++/+ (retrop, pelvic), ++ (inguinal)	—

39	66	F	HGM, NF	NK	Liver (s, large unresect), mesent LN (m), bone (s)	− (liver and LN), + (bone)	—
40	62	M	HGM, NF	Cecum	Liver (4), bone (m)	—	—
41	62	F	LGM, NF	Ileum	Liver (m), bowel prim (3)	+++ (liver), + (bone)	+++ (liver), + (bone)
42	63	M	LGM, sporadic ECL-type, NF	Stomach	Liver (m)	+++	—
43	62	M	LGM, EC-type, F	Ileum	Liver (m), bone (3)	+++ (liver), ++/+++ (bone)	++/+++ (liver), − (bone)
44	66	F	LGM, EC-type, F	NK	Liver (m), mesent LN (m), soft tissue (s)	+++	+++ (liver), ++ (LN), + (soft tissue)
45	60	M	LGM, EC-type, F	Ileum	Liver (m)	+++	+++
46	44	F	LGM, NF	NK	Liver (m)	+++	—
47	40	F	Unspec ICC, LGM, NF	Pancreas	Liver (m), pancr (s)	+++	—
48	54	M	Gastrinoma, LGM, F	Pancreas	Liver (m), bone (m)	+++	—
49	44	M	Gastrinoma, LGM, F	Pancreas	Liver (m), pancr (s)	+++	+++/− (liver), − (pancr)
50	64	M	PPoma, HGM, NF	Pancreas	Liver (m), pancr (s)	++/− (liver), + (pancr)	—
51	63	M	PPoma, LGM, F	Pancreas	Liver (3), pancr (s)	+++	—
52	59	F	Insulinoma, LGM, F	Pancreas	Liver (m), pancr (s), mesent LN (m), mediastinal LN (2)	+++	+++
53	25	M	ICC, mixed exo-/endocrine, LGM, NF	Pancreas	Liver(m), abdom LN (m), medias LN (m)	+++	—
54	71	F	Unspec ICC, LGM, NF	Pancreas	Liver (m), bone (s), pancr (s)	+++	—
55	54	F	Unspec ICC, LGM, NF	Pancreas	Liver (m)	+++	—
56	76	M	Unspec ICC, LGM, NF	Pancreas	Liver (m), abdom LN (m), pancr (s)	+++	− (all; except 1 liver metastases: +++)
57	38	F	Unspec ICC, LGM, NF	Pancreas	Liver (m)	+++	—

HGM = high-grade-malignant; LGM = low-grade-malignant; F = functioning; NF = nonfunctioning; ICC = islet cell carcinoma; NK = not known; s = single; m = multiple; pulm = pulmonary; mesent = mesenteric; LN = lymph node; pancr = pancreatic; abdom = abdominal; medias = mediastinal; retrop = retroperitoneal; unresect = unresected; prim = primary; unspec = unspecified; PPoma = pancreatic polypeptide-secreting tumor; tumoral tracer uptake: − = absent; + = clearly less than liver uptake; ++ = comparable to liver uptake; +++ = clearly more than liver uptake.

2 targeting principles. Because both radiopharmaceuticals can be used for diagnosis as well as for therapy, depending on the radionuclide selected for labeling, the diagnostic scan may serve as a basis for deciding on targeted radionuclide therapy (*2,10,11*). It could be speculated that the influence of a tumor feature on the diagnostic tracer uptake is similar to that on the therapeutic efficiency of the same targeting agent.

Potential relationships between tracer affinity and tumor aspects emphasized by the revised WHO classification—such as primary origin, function, and grade of malignancy—are relevant to both targeting principles. Knowledge of these relations might aid in selecting the appropriate imaging tool and potentially in identifying preferred candidates for targeted therapy and could improve the management of metastatic disease. The aim of this study was to analyze the prevalence of tracer affinity in metastatic GEP-NET from our experience of consecutive dual scintigraphic evaluation with special regard to the morphofunctional aspects. The dual evaluation is based on our clinical approach to test for both Oct and MIBG affinity in patients seeking palliative treatment options, before advising or discouraging specific targeted radionuclide therapy. For the purpose of this study we analyzed the scintigraphic results of 57 consecutive patients. Radionuclide therapy is not considered here and the therapeutic outcome was not included in the analysis because not all patients underwent consecutive targeted radiotherapy, and the selection of the treatment form was influenced by nonmedical facors such as therapy availability and financial reimbursement.

MATERIALS AND METHODS

Tumor Classification

Tumors were classified according to the WHO classification of endocrine tumors (*5*). The histologic examination was performed either on resection specimens ($n = 35$) or biopsy material ($n = 22$). GEP-NET were divided into pancreatic neuroendocrine tumors (P-NET; islet cell carcinomas) and gastroenteral neuroendocrine tumors (GE-NET; formerly termed carcinoid tumors), whereas the term carcinoid was avoided because of its confounding and inconsistent use for either enterochromaffin (EC) cell tumors specifically or non–islet cell GEP tumors (including nonEC cell and poorly differentiated NET) in the broader sense (*12*). Low-grade malignant NET (well-differentiated neuroendocrine carcinoma, type 1b) with a low proliferative index (Ki67-positive cells $\leq 5\%$) were distinguished from high-grade malignant NET (poorly differentiated neuroendocrine carcinoma, type 2); in our study population, all high-grade malignant tumors had proliferation indices ranging between 20% and 75%. The traditional ontogenetically derived carcinoid classification was adapted to distinguish between foregut, midgut, and hindgut GE-NET according to the primary origin. Patients with functioning GEP-NET either had detectable specific hormones (or their metabolites) in serum or urine or exhibited specific symptoms or syndromes, such as flushing or carcinoid syndrome.

Patients

Patients with metastatic NET seeking palliative treatment options were frequently referred to the Department of Nuclear Medicine, University Hospital Bonn for evaluation of targeted radiotherapy options. Our approach has been to test both Oct and MIBG affinity status before advising or discouraging either treatment. For the purpose of this study, we analyzed the results of 57 consecutive patients with metastatic GEP-NET undergoing both scintigraphic studies in this setting.

All 57 patients (mean age, 58 y; age range, 21–79 y; 25 females, 32 males) had histologically confirmed neuroendocrine tumors with metastatic spread that were considered inoperable (no potentially curative surgery). The patient characteristics, tumor features, and location of metastases are given in Table 1. GE-NET included 46 patients (mean age, 59 y; age range, 21–79 y; 20 females, 26 males), of whom 23 had functioning EC cell tumors and 23 had nonfunctioning tumors. Six of the tumors were poorly differentiated (high-grade malignant) and all were nonfunctioning. The primary tumor in the group of GE-NET was undetermined in 11 patients; the remaining cases were classified as midgut ($n = 26$), foregut ($n = 3$), or hindgut ($n = 6$) tumors. P-NET included 11 patients (mean age, 53 y; age range, 25–76 y; 5 females, 6 males), of whom 2 had gastrinoma, 1 had insulinoma, 2 had pancreatic polypeptide-secreting tumor (PPoma) with secretion of pancreatic polypeptide, 1 had a mixed exocrine/endocrine pancreatic tumor that belongs to the group of endocrine pancreatic tumors (*12*), and 5 had unspecified nonfunctioning endocrine pancreatic tumors. Four of the P-NET were functioning; 1 of the nonfunctioning tumors was poorly differentiated. Table 2 lists the frequency of common metastatic sites in the 2 major GEP-NET groups. Overall, 27 patients (47%) had undergone chemotherapy ($n = 11$) or biotherapy with somatostatin analog medication ($n = 22$) or interferon-α ($n = 3$) before imaging.

Imaging

Somatostatin Receptor Scintigraphy. Planar imaging was performed at 4 and 24 h after intravenous injection of 180–220 MBq ^{111}In-pentetreotide (^{111}In-DTPA-D-Phe^1-octreotide; Octreoscan, Mallinckrodt Inc.), including SPECT at 24 h after injection, with a dual head large-field-of-view γ-camera (Prism 2000, Picker) and a medium energy collimator. Additional planar imaging at 48 h postinjection was used for clarification of equivocal abdominal findings. Long-acting somatostatin analog medication was withheld for at least 3 wk before imaging.

MIBG Scintigraphy. Planar imaging was performed at 4 and 24 h after intravenous injection of 250–400 MBq ^{123}I-MIBG (Amersham Health B.V.) and SPECT was performed at 24 h after injection with a dual-head, large-field-of-view γ-camera

TABLE 2
Frequency of Common Metastatic Sites

Site	GE-NET	P-NET	Total
Liver	35 (76.1)	11 (100)	46 (81)
Bone	9 (19.6)	2 (18.1)	11 (19.3)
Lungs	2 (4.3)	0	2 (3.5)
LN	20 (43.5)	3 (27.3)	23 (40.4)

GE-NET = gastroenteral NET; P-NET = pancreatic NET; LN = lymph nodes.

Data are expressed as number of affected patients (percentage in parentheses).

(Prism 2000; Picker International) and a medium-energy collimator ($n = 38$ patients) or planar imaging was performed at 24, 48, and 72 h after intravenous injection of 60–90 MBq ^{131}I-MIBG (Amersham Health B.V.) using a high-energy collimator ($n = 19$ patients). Sufficient time was allowed between ^{111}In-pentetreotide and MIBG scintigraphy to avoid relevant imaging interference (>3 d if ^{111}In-pentetreotide followed ^{123}I-MIBG; otherwise, >14 d).

Analysis of Imaging Results

The intensity of tracer uptake was compared with CT or MRI findings (or both) by 2 experienced nuclear medicine specialists. Semiquantification of tracer affinity in the different metastatic regions was performed by adapting the grading system proposed by Krenning et al. for somatostatin receptor scintigraphy (*13*) to match the conditions of both Oct- and MIBG-based imaging. A 4-point scale was used for grading the tumor uptake at 24 h after injection: 0 or −, absent tumor uptake; 1 or +, clearly less than liver uptake; 2 or ++, comparable to liver uptake; 3 or +++, clearly more than liver uptake. A site- and organ-based evaluation was chosen instead of a lesion-by-lesion analysis for the purpose of the study in view of the prevalence of multiple metastases and disseminated organ involvement. In a second step, each patient was classified as either positive or negative for a tracer. Positivity was defined as uptake of at least grade 2 in clinically relevant tumor lesions; for liver metastases, a grade 3 uptake was required. For example, patients with MIBG-positive liver metastases (grade 3) but not sufficiently positive mesenteric lymph node metastases (grade 0 or 1) were overall classified as MIBG positive.

Statistical Analysis

The χ^2 test or the Fisher exact test (if appropriate) was used for comparison of tracer-positive proportions among different groups of patients. All P values were 2-sided and $P < 0.05$ was considered to be statistically significant. SPSS 12.0 software package was used for statistical calculation.

RESULTS

The detailed results of the scintigraphic studies according to the different metastatic regions are shown in Table 1. Patients were classified as overall positive for a given tracer when clinically relevant tumor lesions displayed sufficient uptake. Patient 32, with multiple, highly Oct-avid, mediastinal lymph node metastases from an aggressive small cell neuroendocrine carcinoma of the rectum, also had multiple liver metastases with no relevant Oct uptake. This patient was classified as Oct positive because the mediastinal metastases were rapidly progressive, causing superior vena cava syndrome, and were, therefore, the determining factor in the treatment. Patient 28 was classified as Oct negative despite sufficient uptake in mesenteric tumor lesions, as the clinically determinant liver metastases showed no relevant tracer accumulation.

With regard to significant overall tracer affinity, 52 of all 57 GEP-NET patients (91.2%) proved positive for Oct, compared with 28 patients (49.1%) positive for MIBG. 7.0% and 10.5% of all patients exhibited only partial or rudimental tracer accumulation of Oct and MIBG, respectively. None of the Oct-negative patients was MIBG positive. Table 3 shows the proportions of tracer-positive patients in different tumor groups.

TABLE 3
Tracer-Positive Patients

Tumor group	*n*	Oct positive	MIBG positive
GEP-NET	57	52 (91.2)	28 (49.1)
GE-NET	46	42 (91.3)	27 (58.7)
P-NET	11	10 (90.9)	1 (9.1)
Foregut GE-NET	3	2 (66.6)	1 (33.3)
Midgut GE-NET	26	23 (96.2)	16 (69.2)
Hindgut GE-NET	6	5 (83.3)	1 (16.7)
GE-NET with undetermined primary	11	10 (90.9)	7 (63.6)
LGM GEP-NET	50	48 (96.0)	28 (56.0)
HGM GEP-NET	7	4 (57.1)	0 (0)
Functional GEP-NET	27	27 (100)	20 (74.1)
Nonfunctional GEP-NET	30	25 (83.3)	8 (26.7)
Nonfunctional LGM GEP-NET	23	21 (91.3)	8 (34.8)
Functional GE-NET with liver metastases	19	19 (100)	17 (89.5)
Nonfunctional LGM GE-NET with liver metastases	10	9 (90)	4 (40)

LGM = low-grade malignant; HGM = high-grade malignant.
Percentage in parentheses.

Figure 1 displays proportions of tracer-positive patients in GEP-NET according to tumor origin. Prevalence of relevant Oct affinity ranges between 77.8% and 96.2%, with no significant differences between the groups. MIBG-positive proportions (9.1% – 69.2%) are lower compared with Oct in all groups, with the highest prevalence seen in midgut GE-NET and GE-NET with unknown primary.

Comparison of radioligand-positive proportions between GE-NET and P-NET (Fig. 2) yields no significant difference for Oct (91.3% vs. 90.9%) but a significant difference for MIBG in favor of the GE-NET group (58.7% vs. 9.1%).

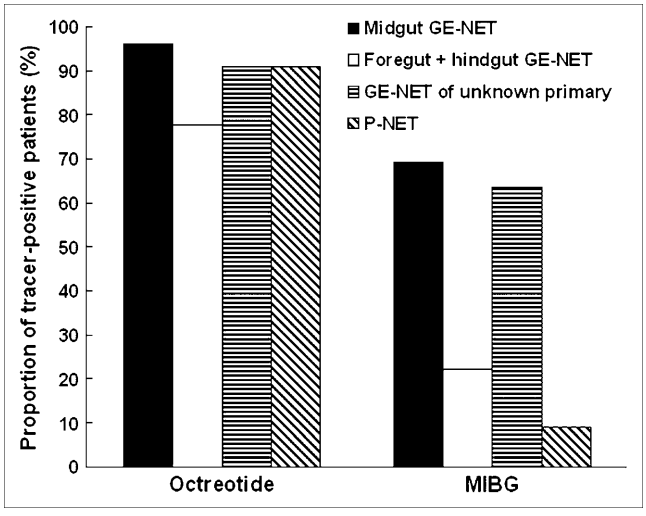

FIGURE 1. Proportions of patients displaying sufficient tracer accumulation with regard to targeted radiotherapy.

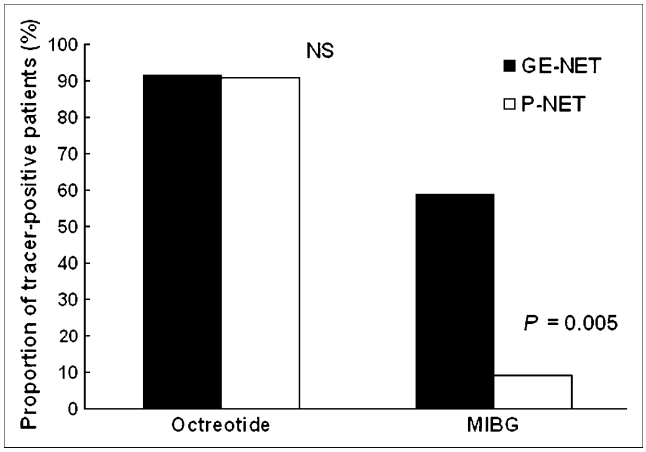

FIGURE 2. Comparison of tracer-positive proportions between GE-NET and P-NET shown for both tracers. NS = not significant.

Figure 3 depicts typical evaluation results of a patient from the P-NET group (patient 56), with strongly Oct-positive tumor lesions and no relevant MIBG uptake overall.

As shown in Figure 4, dichotomizing into high-grade and low-grade malignant GEP-NET produces significantly different proportions of tracer-positive patients ($P = 0.01$) for both Oct (57.1% vs. 96.0%) and MIBG (0% vs. 56.0%). Discrimination between functioning and nonfunctioning GEP tumors (Fig. 5) yields a stronger discrepancy for MIBG than Oct and, after exclusion of high-grade malignant tumors—all of which were nonfunctioning and, therefore, potentially confounding—the difference remains significant for MIBG ($P = 0.01$) but not significant for Oct ($P = 0.207$).

The association of relevant MIBG affinity and functionality is also illustrated for the subgroup of low-grade malignant GE-NET with liver metastases (Fig. 6), where a particularly high proportion of MIBG-positive patients (89.5%) can be seen in the presence of function. Figure 7 gives an example of the dual-tracer avidity in this tumor group, showing the multimodal images of an individual with functioning advanced metastases of a midgut EC cell tumor, a carcinoid tumor in the specific sense of the old nomenclature.

With regard to the potential influence of pretreatment on tracer uptake, Table 4 lists the frequency of radioligand affinity for treated versus untreated patients. The only larger pretreatment group is the one with somatostatin analog medication, showing comparable tracer-positive proportions in treated and untreated individuals. The smaller pretreatment groups ($n = 3$ and $n = 11$) reveal no significant discrepancy. So far, none of the mentioned therapeutic modalities demonstrate a discernible influence on tracer uptake.

DISCUSSION

The individual clinicopathologic profile in GEP-NET based on the revised WHO classification is of therapeutic and prognostic value (*7–9,12*) and warrants comparative studies for diagnostic and therapeutic nuclear medicine. The 2 most advanced methods of molecular imaging and therapeutic targeting of NET are based on MIBG (metabolic tumor targeting) and Oct (somatostatin receptor targeting). Alternative nuclear medicine imaging or therapy approaches for NET involve targeting of other receptors for regulatory peptides—including cholecystokinin/gastrin, bombesin/gastrin-releasing peptide, and vasoactive intestinal peptide or other ways of metabolic targeting—for example, based on iodo-methyltyrosine, Tc-pentavalent dimercaptosuccinic acid (V-DMSA), or ^{18}F-labeled FDG and DOPA (3,4-dihydroxyphenylalanine) for PET (*1*). Radiolabeled Oct and MIBG can both be used for diagnosis as well as for therapy depending on the radionuclide selected for labeling. Potential influencing factors for Oct or MIBG uptake may, thus, have corresponding implications for diagnostic and therapeutic use of the radioligand.

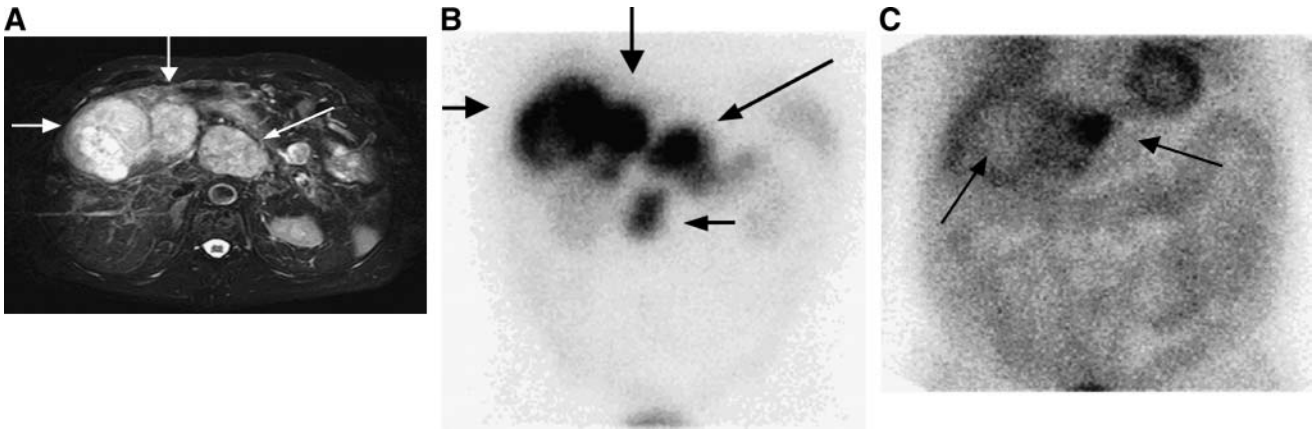

FIGURE 3. MRI (A), ^{111}In-pentetreotide (B), and ^{123}I-MIBG (C) scans of a patient with metastatic nonfunctioning P-NET demonstrate intense Oct uptake in liver and lymph node metastases and the large primary lesion (A and B, arrows). These findings are in contrast to the virtually negative MIBG scan, showing only partial uptake in 1 metastatic lesion in left liver lobe (C, arrow to right), with rest of tumor lesions being negative; note the cold area (C, thin arrow) in the right liver lobe corresponding to the major metastatic site.

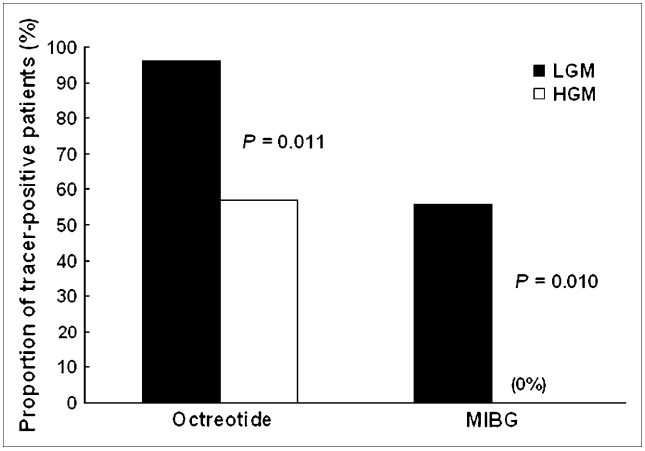

FIGURE 4. Comparison of tracer-positive proportions between low-grade malignant (LGM) and high-grade malignant (HGM) tumors for both tracers. F = functioning; NF = nonfunctioning.

Insight into the relationship between clinicopathologic tumor features and tracer uptake behavior could be relevant for radioimaging-guided patient characterization and tumor staging as well as for potential targeted therapy and should improve patient management. We therefore analyzed the prevalence of diagnostic affinity toward each radioligand in a population of metastatic GEP-NET and examined potential influencing factors for tracer uptake implementing the revised WHO classification of NET.

In our patient population of GEP-NET, scintigraphic evaluation identified 91.2% overall positive for Oct and 49.1% positive for MIBG. Diagnostic sensitivity of Oct and MIBG scintigraphy in GEP-NET is known to range between 78%–100% and 36%–85%, respectively (*2,10,14*). However, the reported data do not refer to a restricted study population with advanced metastatic disease. None of the Oct-negative patients proved to be MIBG positive and half of our patient population displayed dual-tracer avidity.

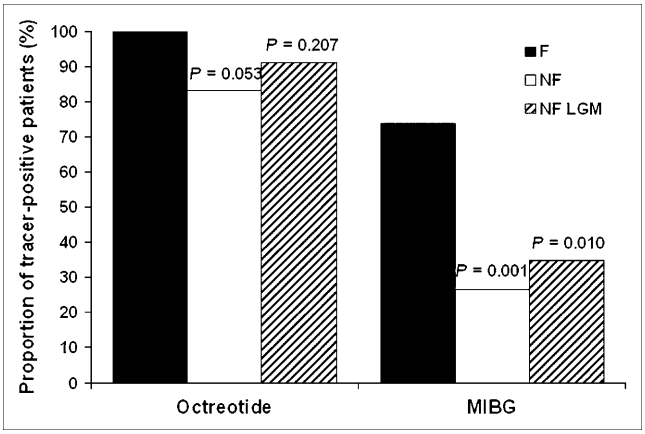

FIGURE 5. Comparison of tracer-positive proportions between functioning (F) and nonfunctioning (NF) GEP-NET for both tracers: low-grade malignant (LGM) NF GEP-NET after exclusion of malignancy for separate analysis of functionality.

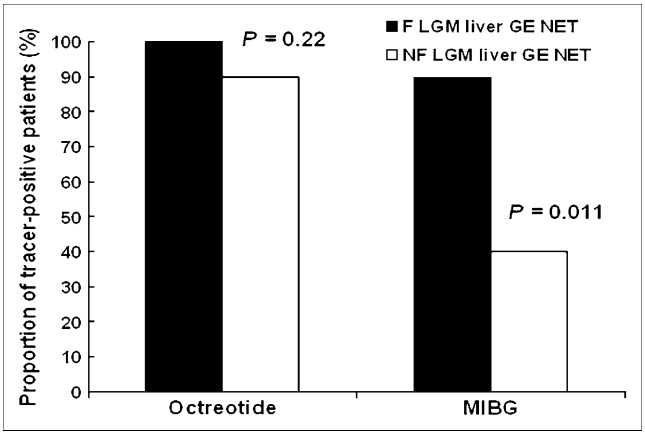

FIGURE 6. Comparison of tracer-positive proportions between functioning (F) and nonfunctioning (NF) low-grade malignant (LGM) GE-NET with liver metastases

Although similar proportions of patients with avid Oct uptake (77.8%–96.2%) were noted throughout the ontogenetically derived subgroups of our patient population, there was a significant discrepancy with regard to MIBG affinity between the nonpancreatic (GE-NET) and pancreatic (P-NET) tumors (58.7% vs. 9.1%), which could not be explained by different distributions of low- and high-grade malignancy or functionality. This finding is consistent with observations of other authors (*2,10,15*), who state the limited use of MIBG in P-NET. The ontogenetically derived groups with the highest proportion of MIBG-positive patients in our study were the midgut GE-NET (69.2%) and the GE-NET with undetermined primary (63.6%). The clinical and prognostic similarity of these 2 tumor groups was described by a larger study on 434 carcinoid tumors (*16*), possibly because the primary tumor in midgut tumors is often difficult to localize (*17*), and a considerable proportion is classified as having an undetermined primary.

Grade of malignancy is increasingly recognized as an important tumor feature in the management of GEP-NET (*17–19*). The WHO classification provides different tumor classes according to malignancy as defined by cell differentiation and proliferation. Two groups of metastatic tumors are distinguished: low-grade malignant GEP-NET (well-differentiated; low-grade neuroendocrine carcinoma) and the less-frequent high-grade malignant GEP-NET (poorly differentiated; high-grade neuroendocrine carcinoma). This histopathologic categorization has prognostic relevance (*8,9*) and aids in decision making and patient management; aggressive treatment such as chemotherapy is generally more efficient and preferred for high-grade rather than low-grade malignant tumors (*17,18,20*). However, to our knowledge, the relationship between grade of malignancy or differentiation and tracer uptake behavior in GEP-NET regarding Oct and MIBG has not adequately been described.

There are observations about the somatostatin receptor status and associated malignancy or prognosis in other tumor types—such as neuroblastoma (*21–25*), medullary

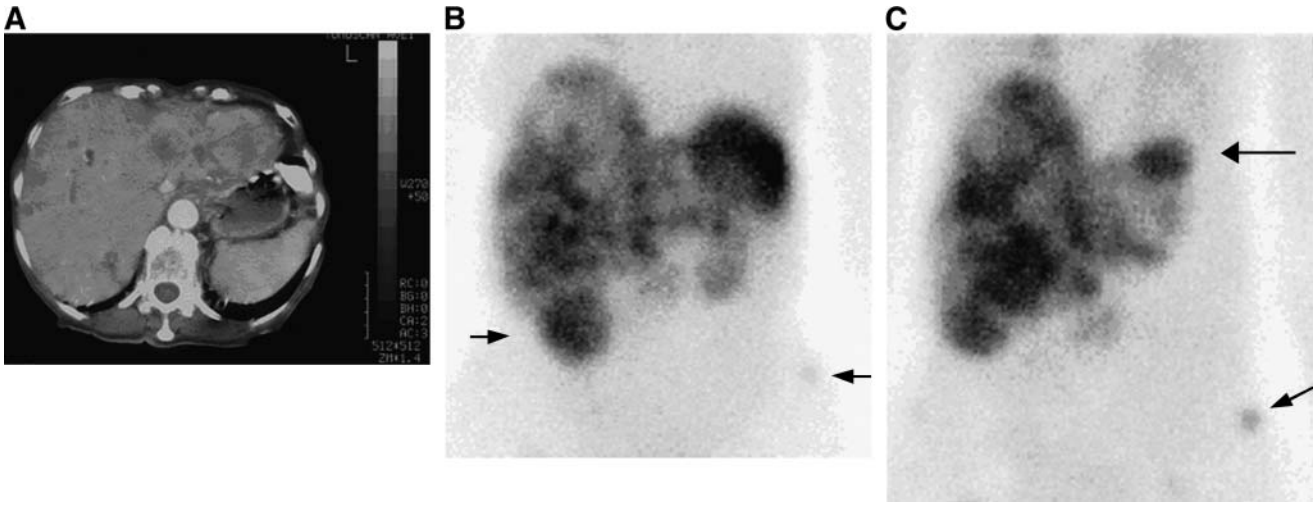

FIGURE 7. CT (A), ^{111}In-pentetreotide (B), and ^{123}I-MIBG (C) images of a patient with advanced functioning EC cell carcinoid disease show multiple metastases to liver and intense uptake of both tracers. Additional site of uptake (B, left arrow) belongs to right kidney. MIBG scan depicts another hepatic lesion (C, upper arrow) obscured in pentetreotide imaging by physiologic splenic uptake. One metastatic pelvic bone lesion (B and C, arrows to lower right) is also better visualized in the MIBG scan.

thyroid carcinoma (*26*), and glioma (*27*)—pointing toward somatostatin receptor loss in tumor cell dedifferentiation. The strongest evidence is for neuroblastoma, where loss of sst2 expression or reduced in vivo detectability via Oct scintigraphy is known to be linked with poor prognosis (*23–25*). In GEP-NET, however, only one early study on human tumor specimens (*28*) weakly indicated a connection between dedifferentiation and lack of somatostatin receptors. Though in vivo studies of somatostatin receptor status through scintigraphy have been well established, no such relationship has been reported (*10,29–32*). This could be either due to a negligible influence of dedifferentiation on somatostatin receptor status or to the lack of discrimination between low-grade and high-grade carcinomas in the analyzed subjects. In our patient population, use of malignancy as a discriminative variable produces a significant association with tracer uptake for both Oct- and MIBG-mediated targeting system ($P = 0.01$). Thus, in addition to a poorer prognosis, high-grade malignant GEP-NET also have a reduced propensity for avid tracer uptake, resulting in reduced efficiency of radioimaging and potentially of targeted radiotherapy. Interestingly, from the clinical point of view, dedifferentiation-induced targeting interference seems less pronounced for Oct, where at least a considerable proportion of patients with high-grade malignant GEP-NET may still prove strongly tracer positive (4/7 patients in our study) compared with MIBG, where none of these patients displayed avid tracer uptake. Future investigations may reveal whether loss of somatostatin receptor overexpression in high-grade malignant GEP-NET is associated with further deterioration of prognosis, as described in other high-grade malignant NET such as neuroblastoma.

TABLE 4
Pretreatment and Proportions of Tracer-Positive Patients

Pretreatment	Status	*n*	Oct positive	MIBG positive
Sandostatin analog medication	Yes	22	21 (95.5)*	12 (54.5)†
	No	35	31 (88.6)*	16 (45.7)†
Chemotherapy	Yes	11	11 (100)‡	3 (27.3)§
	No	46	41 (89.1)‡	25 (54.3)§
Interferon-α	Yes	3	3 (100)‖	2 (66.7)¶
	No	54	49 (90.7)‖	26 (48.1)¶

*$P = 0.639$.
†$P = 0.592$.
‡$P = 0.571$.
§$P = 0.179$.
‖$P = 1.0$.
¶$P = 0.611$.
Percentage in parentheses.

To our knowledge, there is no published work on the relationship of MIBG scintigraphy and grade of malignancy or differentiation in GEP tumors. Our study indicates that high-grade malignancy in GEP-NET is a strong negative predictor of avid MIBG uptake. According to our dual scintigraphic evaluation, it seems that accumulation of MIBG requires a higher level of cell differentiation than that needed for the overexpression of somatostatin receptors. Because MIBG uptake correlates with the extent of intracellular neurosecretory granules in chromaffin tumors (*33*), this suggests that cytomorphologic structures responsible for uptake and storage are more easily lost in the process of dedifferentiation in GEP-NET. This might support the recent finding that high initial activities applied in ^{131}I-MIBG therapy of carcinoid tumors are linked with prolonged survival (*34*), possibly because higher tumor doses are achieved before fractional dedifferentiation

occurs. The fact that chromogranin A is not usually found in high-grade malignant specimens in contrast to low-grade malignant GEP-NET (*18*), might be associated with the failure to sufficiently concentrate MIBG in these tumors. In this context, the recent work of a Swedish group (*35*) on the role of vesicular monoamine transporter (VMAT) 1 and 2 for MIBG uptake in GEP-NET should be mentioned, pointing to potential future histopathologic prediction of tracer affinity.

The impact of tumor functionality on tracer uptake in GEP-NET is not well established. In a larger study (*29*), diagnostic Oct uptake was not dependent on the presence or absence of hormone secretion in carcinoid tumors. In smaller series comparing diagnostic Oct and MIBG uptake in metastatic GEP-NET and carcinoid tumors, few distinctions were observed between the influence on Oct and MIBG uptake. These studies described either a significantly higher rate of positive scans for both tracers in functioning compared with nonfunctioning tumors (*36*) or only for MIBG in patients with flush compared with those without (*37*); no significant correlation was found between functionality and uptake of both tracers (*38*). In our work, to independently evaluate functionality we first excluded the high-grade malignant tumors, which were all nonfunctioning and, therefore, potentially confounding. As a result, functionality in GEP-NET did not significantly impact the prevalence of Oct affinity, whereas it was significantly associated with MIBG uptake ($P < 0.01$). Functioning tumors were more likely to display avid uptake than nonfunctioning tumors (74.1% vs. 37.8%). However, in the clinical setting, where a patient with a nonfunctioning metastatic GEP tumor may harbor an unidentified poorly differentiated neuroendocrine carcinoma, functionality (e.g., the presence of carcinoid syndrome) provides to some extent an exclusion of high-grade malignancy (*18*), and in that way represents a positive predictive factor of radioligand accumulation for both agents, though not independent and only borderline significant in the case of Oct ($P = 0.053$).

The highest prevalence of MIBG affinity was observed in functioning EC cell carcinoid metastases, with almost 90% of patients exhibiting efficient tracer uptake. This is encouraging for the diagnostic use and presumably also with regard to ^{131}I-MIBG therapy, which might be frequently considered possible in this patient group. Because MIBG-positive patients displayed strong Oct affinity as well, this tumor group offers also the highest rate of dual-tracer avidity in GEP-NET, which supports dual imaging in case of equivocal somatostatin receptor scintigraphy findings. Furthermore, if combined targeted radionuclide therapy has the potential to provide higher tumor radiation doses with limited renal toxicity, this GE-NET subgroup may prove well suited for dual-targeting approaches. MIBG accumulation is particularly meaningful in functioning EC cell carcinoid tumors because these patients can be offered sustained symptom control with MIBG therapy (*39,40*). On the other hand, nonfunctioning tumors may also benefit from MIBG treatment in terms of increased survival, as suggested by recent studies (*34,41*). However, our results indicate that avid MIBG uptake in the diagnostic scan is significantly less likely in nonfunctioning GE-NET. Even after exclusion of high-grade malignant tumors (which were all MIBG negative), the proportion of strongly MIBG-positive patients dropped from 89.5% in functioning EC cell carcinoid tumors with liver metastases to 40% in those without function. Thus, absence of any functional symptoms or detectable specific hormones (serotonin or metabolite 5-HIAA) seems to significantly impair MIBG imaging of metastatic well-differentiated GE-NET. It appears probable that the a priori chances of feasible MIBG therapy are affected in the same way. Future studies may investigate the potential impact of tumor functionality on MIBG therapy. However, one should keep in mind that 40% of the patients with nonfunctioning nondedifferentiated GE-NET are still strongly MIBG positive. Compared with its role in our study, functionality is generally regarded less important for MIBG uptake in pheochromocytoma and paraganglioma (*2,10,42*), where only the catecholamine storage capacity, but not the secretion (i.e., function), was shown to strongly correlate with MIBG uptake (*33*).

For the somatostatin receptor-targeting system, represented by ^{111}In-pentetreotide in our study, there is overall more homogeneity of affinity prevalence throughout most subgroups of GEP-NET. The only significant influencing factor is grade of malignancy, whereas tumor function revealed no significant independent impact on in vivo somatostatin receptor status. The presence of functionality only provided indirect positive prediction of Oct accumulation by clinical exclusion of high-grade malignancy, and even this effect was only borderline significant ($P = 0.053$).

The variable use of ^{123}I- and ^{131}I-labeled MIBG in our series might have influenced the results and, thus, the conclusions drawn. Whereas ^{123}I-MIBG yields better image quality and clearer tumor delineation, the diagnostic use of ^{131}I-MIBG is still accepted (*43*) and, in our opinion, is particularly suitable for the purpose of assessing tumor affinity, as applied in our study. However, our data show no correlation between the radionuclide used and the documented MIBG affinity ($P = 0.86$). Prior treatment with somatostatin analog medication or chemotherapy did not show a discernible impact on either Oct or MIBG accumulation. The small patient number pretreated with interferon-α ($n = 3$) did not permit respective inference.

We quantified the tracer-positive patients and potentially influencing morphofunctional features by examining the results of our standard dual scintigraphic evaluation in metastatic GEP-NET. Because of this approach, the study population consisted only of individuals who were examined with both modalities. Therefore, the subjects for Oct and MIBG analyses were identical and different results for Oct and MIBG were not attributable to different patient characteristics in the analyzed groups.

The study population size in this heterogeneous tumor entity was not large enough to explore other variables, and the number of patients in subgroups such as the foregut and hindgut tumors or different pancreatic tumor subgroups (as insulinoma or gastrinoma) was too small to perform additional analyses or infer further conclusions. The problem of low tumor incidence represents a general difficulty for scientific investigations in GEP-NET, and, to out knowledge, the largest Oct MIBG dual-tracer studies published represent small patient series (*15,36–38*) with up to 36 GEP-NET (*15*).

CONCLUSION

Our retrospective dual-tracer study in inoperable metastatic GEP-NET revealed no case with overall exclusive binding of MIBG (i.e., Oct negative but MIBG positive). We found high prevalence of strong affinity for radiolabeled octreotide throughout the GEP groups with the only significant negative influencing factor being dedifferentiation of tumors—that is, high-grade carcinomas. Corresponding MIBG uptake is overall less prevalent and more group dependent and, notably, of limited use in endocrine pancreatic tumors. Both function and grade of malignancy represent significant independent influencing factors for MIBG accumulation, which is particularly prevalent in functioning GE-NET—that is, secreting EC cell tumors. This group is best suited for additional or confirmatory MIBG imaging and presumably may frequently show individuals eligible for ^{131}I-MIBG therapy, besides the highly efficient somatostatin receptor imaging system. In contrast to this tumor group, somatostatin receptor targeting seems to be the only remaining of the 2 methods in endocrine pancreatic tumors and high-grade carcinomas; these tumors should, thus, be evaluated only by somatostatin receptor scintigraphy. Further implications for patient management and potentially for selection and performance of targeted therapy are left to be demonstrated by future investigations.

REFERENCES

1. Li S, Beheshti M. The radionuclide molecular imaging and therapy of neuroendocrine tumors. *Curr Cancer Drug Targets.* 2005;5:139–148.
2. Kaltsas GA, Mukherjee JJ, Grossman AB. The value of radiolabelled MIBG and octreotide in the diagnosis and management of neuroendocrine tumours. *Ann Oncol.* 2001;12(suppl):47–50.
3. Ahlman H, Nilsson O. The gut as the largest endocrine organ in the body. *Ann Oncol.* 2001;12(suppl):63–68.
4. Barakat MT, Meeran K, Bloom SR. Neuroendocrine tumours. *Endocr Relat Cancer.* 2004;11:1–18.
5. Solcia E, Kloppel G, Sobin LH, et al. *Histological Typing of Endocrine Tumours: WHO International Histological Classification of Tumours*. 2nd ed. Berlin, Germany: Springer; 2000.
6. Rindi G, Kloppel G. Endocrine tumors of the gut and pancreas tumor biology and classification. *Neuroendocrinology.* 2004;80(suppl):12–15.
7. Rindi G, Capella C, Solcia E. Introduction to a revised clinicopathological classification of neuroendocrine tumors of the gastroenteropancreatic tract. *Q J Nucl Med.* 2000;44:13–21.
8. Schindl M, Kaczirek K, Kaserer K, Niederle B. Is the new classification of neuroendocrine pancreatic tumors of clinical help? *World J Surg.* 2000;24:1312–1318.
9. Bruwer M, Pahlov-Nejad T, Herbst H, Senninger N, Schurmann G. Neuroendocrine tumors of the gastroenteropancreatic system: reevaluation using the Capella classification. *Zentralbl Chir.* 2003;128:656–662.
10. Hoefnagel CA. Metaiodobenzylguanidine and somatostatin in oncology: role in the management of neural crest tumours. *Eur J Nucl Med.* 1994;21:561–581.
11. Krenning EP, Kwekkeboom DJ, Valkema R, Pauwels S, Kvols LK, De Jong M. Peptide receptor radionuclide therapy. *Ann N Y Acad Sci.* 2004;1014:234–245.
12. Kloppel G, Perren A, Heitz PU. The gastroenteropancreatic neuroendocrine cell system and its tumors: the WHO classification. *Ann N Y Acad Sci.* 2004;1014:13–27.
13. Krenning EP, Valkema R, Pauwels S, et al. Radiolabeled somatostatin analogue(s): peptide receptor scintigraphy and radionuclide therapy. In: Mignon M, Colombel JF, eds. *Recent Advances in the Pathophysiology and Management of Inflammatory Bowel Diseases and Digestive Endocrine Tumors.* Paris, France: John Libbey Eurotext; 1999:220–228
14. Krenning EP, Kwekkeboom DJ, Pauwels S, Kvols LK, Reubi JC. Somatostatin receptor scintigraphy. In: Freeman L, ed. *Nuclear Medicine Annals.* New York, NY: Raven Press; 1995:1–50.
15. Kaltsas G, Korbonits M, Heintz E, et al. Comparison of somatostatin analog and meta-iodobenzylguanidine radionuclides in the diagnosis and localization of advanced neuroendocrine tumors. *J Clin Endocrinol Metab.* 2001;86:895–902.
16. Kirshbom PM, Kherani AR, Onaitis MW, Feldman JM, Tyler DS. Carcinoids of unknown origin: comparative analysis with foregut, midgut, and hindgut carcinoids. *Surgery.* 1998;124:1063–1070.
17. Kaltsas GA, Besser GM, Grossman AB. The diagnosis and medical management of advanced neuroendocrine tumors. *Endocr Rev.* 2004;25:458–511.
18. de Herder WW, Krenning EP, Van Eijck CH, Lamberts SW. Considerations concerning a tailored, individualized therapeutic management of patients with (neuro)endocrine tumours of the gastrointestinal tract and pancreas. *Endocr Relat Cancer.* 2004;11:19–34.
19. Krenning EP, Valkema R, Kwekkeboom DJ, et al. Molecular imaging as in vivo molecular pathology for gastroenteropancreatic neuroendocrine tumors: implications for follow-up after therapy. *J Nucl Med.* 2005;46(suppl):76–82.
20. O'Toole D, Hentic O, Corcos O, Ruszniewski P. Chemotherapy for gastroenteropancreatic endocrine tumours. *Neuroendocrinology.* 2004;80(suppl):79–84.
21. Moertel CL, Reubi JC, Scheithauer BS, Schaid DJ, Kvols LK. Expression of somatostatin receptors in childhood neuroblastoma. *Am J Clin Pathol.* 1994;102:752–756.
22. Schilling FH, Ambros PF, Bihl H, et al. Absence of somatostatin receptor expression in vivo is correlated to di- or tetraploid 1p36-deleted neuroblastomas. *Med Pediatr Oncol.* 2001;36:56–60.
23. Schilling FH, Bihl H, Jacobsson H, et al. Combined ^{111}In-pentetreotide scintigraphy and ^{123}I-mIBG scintigraphy in neuroblastoma provides prognostic information. *Med Pediatr Oncol.* 2000;35:688–691.
24. Orlando C, Raggi CC, Bagnoni L, et al. Somatostatin receptor type 2 gene expression in neuroblastoma, measured by competitive RT-PCR, is related to patient survival and to somatostatin receptor imaging by indium-111-pentetreotide. *Med Pediatr Oncol.* 2001;36:224–226.
25. Raggi CC, Maggi M, Renzi D, et al. Quantitative determination of sst2 gene expression in neuroblastoma tumor predicts patient outcome. *J Clin Endocrinol Metab.* 2000;85:3866–3873.
26. Reubi JC, Chayvialle JA, Franc B, Cohen R, Calmettes C, Modigliani E. Somatostatin receptors and somatostatin content in medullary thyroid carcinomas. *Lab Invest.* 1991;64:567–573.
27. Reubi JC, Horisberger U, Lang W, Koper JW, Braakman R, Lamberts SW. Coincidence of EGF receptors and somatostatin receptors in meningiomas but inverse, differentiation-dependent relationship in glial tumors. *Am J Pathol.* 1989;134:337–344.
28. Reubi JC, Kvols LK, Waser B, et al. Detection of somatostatin receptors in surgical and percutaneous needle biopsy samples of carcinoids and islet cell carcinomas. *Cancer Res.* 1990;50:5969–5977.
29. Krenning EP, Kwekkeboom DJ, Bakker WH, et al. Somatostatin receptor scintigraphy with [^{111}In-DTPA-D-Phe1]- and [^{123}I-Tyr3]-octreotide: the Rotterdam experience with more than 1000 patients. *Eur J Nucl Med.* 1993;20:716–731.
30. Schillaci O, Spanu A, Scopinaro F, et al. Somatostatin receptor scintigraphy in liver metastasis detection from gastroenteropancreatic neuroendocrine tumors. *J Nucl Med.* 2003;44:359–368.
31. Schillaci O, Spanu A, Scopinaro F, et al. Somatostatin receptor scintigraphy with ^{111}In-pentetreotide in non-functioning gastroenteropancreatic neuroendocrine tumors. *Int J Oncol.* 2003;23:1687–1695.

32. Krenning EP, Kwekkeboom DJ, Oei HY, et al. Somatostatin-receptor scintigraphy in gastroenteropancreatic tumors. an overview of European results. *Ann N Y Acad Sci.* 1994;733:416–424.
33. Bomanji J, Levison DA, Flatman WD, et al. Uptake of iodine-123 MIBG by pheochromocytomas, paragangliomas, and neuroblastomas: a histopathological comparison. *J Nucl Med.* 1987;28:973–978.
34. Safford SD, Coleman RE, Gockerman JP, et al. Iodine-131 metaiodobenzylguanidine treatment for metastatic carcinoid. results in 98 patients. *Cancer.* 2004; 101:1987–1993.
35. Nilsson O, Jakobsen AM, Kolby L, Bernhardt P, Forssell-Aronsson E, Ahlman H. Importance of vesicle proteins in the diagnosis and treatment of neuroendocrine tumors. *Ann N Y Acad Sci.* 2004;1014:280–283.
36. Taal BG, Hoefnagel CA, Valdes Olmos RA, Boot H. Combined diagnostic imaging with ^{131}I-metaiodobenzylguanidine and ^{111}In-pentetreotide in carcinoid tumours. *Eur J Cancer.* 1996;32:1924–1932.
37. Nocaudie-Calzada M, Huglo D, Carnaille B, Proye C, Marchandise X. Comparison of somatostatin analogue and metaiodobenzylguanidine scintigraphy for the detection of carcinoid tumours. *Eur J Nucl Med.* 1996;23:1448–1454.
38. Ramage JK, Williams R, Buxton-Thomas M. Imaging secondary neuroendocrine tumours of the liver: comparison of I123 metaiodobenzylguanidine (MIBG) and In111-labelled (Octreoscan). *QJM.* 1996;89:539–542.
39. Taal BG, Hoefnagel CA, Valdes Olmos RA, Boot H, Beijnen JH. Palliative effect of metaiodobenzylguanidine in metastatic carcinoid tumors. *J Clin Oncol.* 1996;14:1829–1838.
40. Pathirana AA, Vinjamuri S, Byrne C, Ghaneh P, Vora J, Poston GJ. ^{131}I-MIBG radionuclide therapy is safe and cost-effective in the control of symptoms of the carcinoid syndrome. *Eur J Surg Oncol.* 2001;27:404–408.
41. Sywak MS, Pasieka JL, McEwan A, Kline G, Rorstad O. ^{131}I-Metaiodobenzylguanidine in the management of metastatic midgut carcinoid tumors. *World J Surg.* 2004;28:1157–1162.
42. Van der Harst E, de Herder WW, Bruining HA, et al. [^{123}I]Metaiodobenzylguanidine and [^{111}In]octreotide uptake in benign and malignant pheochromocytomas. *J Clin Endocrinol Metab.* 2001;86:685–693.
43. Bombardieri E, Aktolun C, Baum RP, et al. ^{131}I/^{123}I-Metaiodobenzylguanidine (MIBG) scintigraphy: procedure guidelines for tumour imaging. *Eur J Nucl Med Mol Imaging.* 2003;30:BP132–BP139.